Nuclear Materials and Energy 47 (2026) 102105

Contents lists available at ScienceDirect

Nuclear Materials and Energy

journal homepage: www.elsevier.com/locate/nme

Dissolution of deuterium into Pb-Li and determination of the Sieverts' constant

Ester Diaz-Alvarez [a,b,*], Rodrigo Antunes [c], Stefan Welte [a], Laëtitia Frances [a]

[a] Tritium Laboratory Karlsruhe, Karlsruhe Institute of Technology, Hermann-von-Helmholtz-Platz 1, 76344 Eggenstein-Leopoldshafen, Germany
[b] CIEMAT-Laboratorio Nacional de Fusión, Avda. Complutense 40, 28040 Madrid, Spain
[c] Max Planck Institute for Plasma Physics, Boltzmannstrasse 2, 85748 Garching b. München, Germany

ARTICLE INFO

Keywords:
Eutectic lead–lithium
Solubility
Tritium
Liquid breeding blanket
Tritium extraction and removal system

ABSTRACT

The development of liquid breeding blanket technologies for ITER and DEMO, based on eutectic Pb-Li, faces significant challenges due to the unknown solubility of hydrogen isotopes in Pb-Li. Reported values in the literature span several orders of magnitude, creating substantial uncertainty in experimental design and data interpretation of Tritium Extraction and Removal System (TERS) technologies. In this work, deuterium is dissolved into eutectic Pb-Li using a stationary method and quantified via a mass balance analysis performed at the point of steady-state. The average atomic deuterium concentrations dissolved in Pb-Li are 1.5 ± 0.3 and 0.7 ± 0.2mol m^{-3}, at dissolving pressures of 947 and 472 hPa, respectively, and 673 K. The obtained Sieverts' constant, (4.3 ± 1.1) × 10^{-3} mol m^{-3} $Pa^{-1/2}$ at 673 K, is determined considering deuterium permeation through the chamber walls and with a known Pb-Li composition of 15.2 ± 0.2 at.% Li. This value is presented with a rigorous uncertainty analysis and widely discussed with regard to previously reported data in the literature.

1. Introduction

The liquid breeding blanket concept to be tested in ITER, Water Cooled Lithium-Lead (WCLL), as well as other liquid candidates for the EU-DEMO, Helium Cooled Lithium-Lead (HCLL) and Dual Coolant Lithium-Lead (DCLL), rely on the Pb-Li alloy to generate the tritium required to fuel the fusion plasma [1–3]. The eutectic mixture, 15.7 at.% Li [4,5], is used due to its minimum melting point (at 508 K).

Experimental research on breeding blanket technologies, particularly the validation of Tritium Extraction and Recovery Systems (TERS), presents significant challenges. Operating with Pb-Li and hydrogen isotopes requires an environment free of oxygen and water, high temperatures, and materials that are compatible with Pb-Li and, eventually, tritium. Moreover, one of the major obstacles in TERS development is the wide discrepancy in reported solubility values of hydrogen isotopes in eutectic Pb-Li in literature, spanning several orders of magnitude (see Fig. 7) [6–20]. Reasons for the reported discrepancies have been examined in previous review studies [21–23], which primarily concluded the following:

- The method used to determine the Sieverts' constant significantly influences the results. Typically, absorption methods yield higher values than permeation methods, while desorption methods tend to produce even lower solubility values.
- The solubility of hydrogen isotopes increases with the lithium concentration in the Pb-Li allow.
- The complete chemical composition of Pb-Li, including trace impurities, also affects solubility measurements. However, composition analyses are not often reported in published studies.

In this work, we present a detailed method for dissolving deuterium in Pb-Li, in the framework of experimental validation of TERS techniques. The experimental results include the quantification of dissolved deuterium and the corresponding Sieverts' constant, together with a composition analysis of the Pb-Li alloy. These results stem from a carefully designed experimental strategy, a methodical evaluation of deuterium permeation into the structural materials (which is rarely reported), and a rigorous uncertainty analysis.

2. Experimental facility and Pb-Li

2.1. The experimental facility

An experimental facility, described in [24] and operated with

* Corresponding author at: CIEMAT-Laboratorio Nacional de Fusión, Avda. Complutense 40, 28040 Madrid, Spain.
E-mail address: ester.diaz@ciemat.es (E. Diaz-Alvarez).

https://doi.org/10.1016/j.nme.2026.102105
Received 24 November 2025; Received in revised form 29 January 2026; Accepted 23 March 2026
Available online 25 March 2026

deuterium (D_2), was built at the TLK to investigate one TERS technique, the Vacuum Sieve Tray (VST). It features two chambers, one to perform the dissolution and another one for the extraction, both connected by two pipes to close the Pb-Li loop. This facility was used to study the dissolution process, which is crucial to reliably determine the amount of deuterium dissolved (and ultimately an extraction efficiency).

The dissolution chamber, made of stainless steel 316 L, has dimensions of 0.25 m in diameter and 0.095 m in height (see Fig. 1). It is designed to maximise the gas–liquid interface thereby favouring the dissolution process. The internal volume has been measured with a high accuracy method [25] to be $(4.88 \pm 0.02) \times 10^{-3}$ m^3.

A pressure sensor, RP-01, of full-scale 3×10^5 Pa (model PTA227, EFE), is positioned at a cold finger due to its working temperature limitation, and has an uncertainty of $\pm$ 1.08 hPa (after accounting for calibrations of the sensitivity shifts with temperature). To measure the gas and liquid metal temperature, and the Pb-Li height, five thermocouples (K type) are positioned at different heights in the chamber (see RT-01 – RT-05 in Fig. 1). During the dissolution, RT-01 and RT-02 measure the gas temperature while the sensors RT-03 and RT-04 are immersed in Pb-Li.

2.2. The lead–lithium

15.10 kg of Pb-Li (99.95% purity, 15.7 at.% Li), supplied by the company CAMEX, spol. s r. o., were introduced into the dissolution chamber, in form of ingots, after undergoing a sanding process to remove any oxide layer. From the moment the chamber was closed until the first dissolution experiment, the Pb-Li was under evacuation during four weeks at 453 K and the subsequent three weeks at 673 – 713 K, with argon flushing cycles (during the commissioning of the setup), to eliminate any possible remaining oxides. The composition of the Pb-Li was analysed after the experimental campaign by the Chemical Analysis group in IAM-AWP, KIT, with inductively coupled plasma atomic emission spectroscopy (ICP-AES). Table 1 shows the results of the composition analysis.

The lithium content (also analysed prior to the experimental campaign) was found to be inhomogeneous. Thus, the deviation from the eutectic point, with a measured lithium concentration of 0.592 wt% (15.2 $\pm$ 0.2 at.%), is attributed to the incomplete homogeneity of the provided mixture. Additionally, the melting point of the ingots inserted in the facility, in the range of 511 – 513 K, is in agreement with the atomic concentration 15.2 at.% Li, from the Pb-Li phase diagram reported by Hubberstey *et al.* [5]. It is important to note that a small deviation in the atomic concentration of lithium (and inhomogeneity) seems to be a common issue in the manufacturing of eutectic Pb-Li [21]. This may be explained by the low atomic concentration of Li and the large difference of atomic mass with respect to Pb.

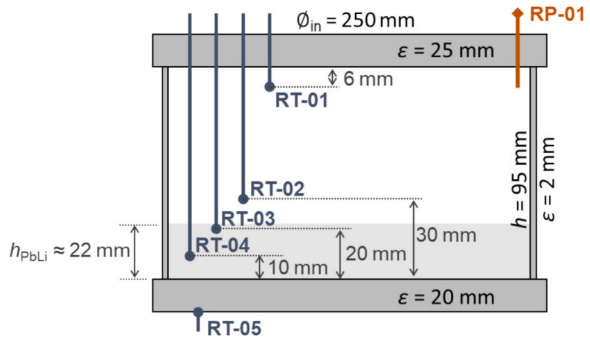

Fig. 1. The dissolution chamber dimensions and position of pressure (RP) and temperature (RT) sensors.

Table 1
Composition analysis of the Pb-Li after the experimental campaign (2500 h molten). The combined mean values and standard deviations (SD) are calculated from two samples, analysed at three positions each. Ti, Zn, Ag, Sn, Sb were also analysed and found below detection levels.

Element	Unit	Mean value	SD
Li	wt.%	0.592	0.033
Cr	wt.%	<0.001	0.0003
Mn	wt.%	<0.001	0.00004
Fe	wt.%	0.001	0.002
Ni	wt.%	0.004	0.0009
Cu	wt.%	0.001	0.0005
Pb	wt.%	98.80	0.14
Bi	wt.%	0.005	0.004
Total:	wt.%	99.404	

3. Methodology

3.1. Procedure and evaluation of D_2 dissolved

The dissolution procedure consists in introducing D_2 into the dissolution chamber, containing the liquid Pb-Li, up to a desired pressure. With the chamber sealed, the pressure decrease, due to dissolution of D_2 into the Pb-Li, and temperature are monitored over 48 h. According to Sieverts' law, D_2 molecules dissociate on the liquid metal surface and dissolve as atomic deuterium. When equilibrium is reached, the atomic concentration of deuterium (in mol$_D$ m^{-3}) is theoretically defined by:

$$C_D = K_s \sqrt{p_{D_2}} \quad (1)$$

where p_{D2} represents the partial pressure of D_2 in the gas phase (in Pa), and K_s is the solubility coefficient or Sieverts' constant (in mol$_D$ m^{-3} Pa$^{-1/2}$). In this study, the concentration is determined from the pressure decrease in the chamber (as explained below), and the Sievert's constant is calculated with equation (1).

During a typical dissolution experiment, the amount of D_2 gas initially inserted in the chamber decreases over time due to its diffusion into both the liquid Pb-Li and the stainless-steel walls, as shown in Fig. 2 a). Once the equilibrium in the Pb-Li is reached (hereafter referred to as τ_{diss}), the amount of deuterium dissolved in the Pb-Li, $n_{D2[PbLi]}$, cannot be accurately calculated using Sieverts' law due to the aforementioned discrepancy in literature values. Instead, a mass balance in the gas phase

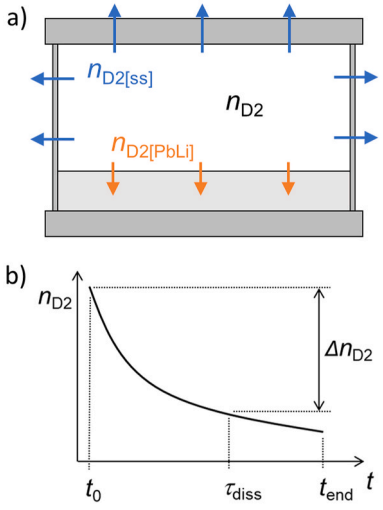

Fig. 2. a) scheme of a dissolution experiment, depicting amount of d_2 gas in the chamber (n_{D2}), D_2 lost through the non-wetted walls ($n_{D2[ss]}$) and D_2 dissolved into Pb-Li ($n_{D2[PbLi]}$). b) Time evolution of D_2 gas in the chamber, with Δn_{D2} being the amount of D_2 that has entered both Pb-Li and stainless-steel walls until τ_{diss}.

is employed to quantify the deuterium dissolved in Pb-Li, as follows:

$$-\Delta n_{D2} = n_{D2[ss]} + n_{D2[PbLi]} \quad (2)$$

where $-\Delta n_{D2}$ refers to the variation of D_2 in the gas phase in the chamber, as shown in Fig. 2 b); $n_{D2[ss]}$ is the amount of D_2 lost through the stainless-steel walls of the chamber, and $n_{D2[PbLi]}$ is the amount of D_2 dissolved into the Pb-Li. $n_{D2[PbLi]}$ is determined following four main steps:

1. Evaluation of the time at which equilibrium inside the Pb-Li is reached (τ_{diss}). This is considered to be the dissolution time. Beyond τ_{diss} the Pb-Li is saturated, i.e., the deuterium net flux is zero: atoms that enter the liquid metal, also leave it through the wetted surfaces [26]. Therefore, the mass balance to determine the deuterium dissolved has to be evaluated at τ_{diss}. The present approach assumes that before τ_{diss} no D_2 (or a negligible amount) escapes the liquid metal.
2. Evaluation of the total amount of gas lost into Pb-Li and stainless steel until τ_{diss} (Δn_{D2}). With the time evolution of pressure and temperature of the D_2 gas inside the chamber, the curve $n_{D2}(t)$, as in Fig. 2 b), is obtained with the ideal gas law (equation (4)). Δn_{D2} is the difference between the initial amount, $n_{D2}(t_0)$, and $n_{D2}(\tau_{diss})$.
3. Evaluation of the amount of D_2 permeated through the walls ($n_{D2[ss]}$). It involves the following steps:
   a. Permeation experiments without Pb-Li are done to determine experimentally the D_2 that permeates through the whole chamber under the same conditions of p and T as those used during the dissolution phase (Fig. 3 a)). Note that the obtained amount $n_{D2[ss*]}$ is marked with an asterisk to denote permeated through all the walls (to distinguish it from $n_{D2[ss]}$, which denotes permeation only through the non-wetted walls, as in Fig. 2 a).
   e. The percentage of D_2 permeated through the top surfaces 1 and 2 in Fig. 3 b) (χ_{top}) corresponds to the non-wetted walls in a dissolution experiment. χ_{top} is theoretically calculated using the literature data of permeability for stainless steel, the thicknesses of the walls and their temperature profile, as shown in Fig. 3 b).
   f. χ_{top} is applied to the experimental total value $n_{D2[ss*]}$ above calculated (a.) to obtain the amount of D_2 that permeates through the non-wetted walls in the dissolution experiments, $n_{D2[ss]}$, as follows:

$$n_{D2[ss]} = \chi_{top} n_{D2[ss*]} \quad (3)$$

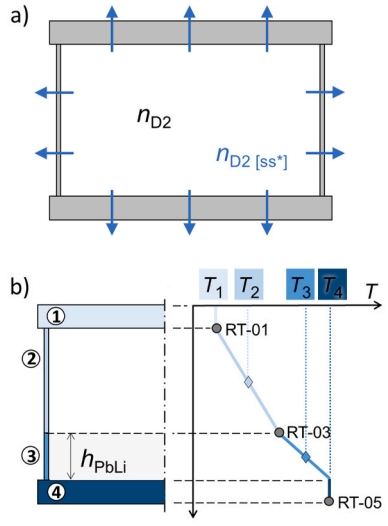

Fig. 3. a) scheme of a permeation experiment (without pb-li), depicting the amount of d_2 lost through the walls ($n_{D2[ss*]}$). b) Temperature profile used in the permeation calculations at the four permeation sections, 1: upper flange, 2: non-wetted wall, 3: wetted wall, and 4: wetted lower flange. T_2 and T_3 are interpolated from the measured temperatures RT-01, RT-03 and RT-05.

4. Determination of the amount of deuterium dissolved in the Pb-Li ($n_{D2[PbLi]}$), with equation (2).

In order to ensure repeatability and to verify the leak-tightness of the dissolution chamber, the following procedure was carried out between experiments:

1. The Pb-Li is drained from the dissolution chamber to another chamber.
2. A four-day long bake-out is performed to the whole setup at 723 K with active evacuation.
3. The Pb-Li is recirculated back into the dissolution chamber.
4. Thermalization until the operation temperature (673 K) is achieved after 6 h, with continuous evacuation.
5. A 16-hour vacuum test with the chamber closed is conducted to verify a leak rate below 6×10^{-5} mbar l/s.

The same procedure is followed for the experiments without Pb-Li (without steps 1 and 3).

This procedure conducted before each experiment guarantees that the pressure decrease is only due to dissolution into Pb-Li and permeation through the stainless-steel chamber walls.

3.2. Experimental campaign

The experimental campaign is divided into two sets:

(i) First, three permeation experiments without Pb-Li (as in Fig. 3) were conducted. Two of them, at an initial pressure of $p_{D2} = 1000$ hPa, were performed to verify repeatability, and a third experiment was carried out at $p_{D2} = 500$ hPa. The heater at the bottom of the chamber was kept at 684 K in order to maintain a temperature profile in the chamber as close as possible to the one in the dissolution experiments.

(ii) Afterwards, the Pb-Li was introduced in the chamber and six dissolution experiments (as in Fig. 2) were performed. Runs #01, #02, #03 and #06 were conducted at an initial gas pressure $p_{D2} = 1000$ hPa, and runs #04 and #05 start at $p_{D2} = 500$ hPa. All experiments were performed at $T_{PbLi} = 673$ K and at a dissolution time of 48 h.

3.3. Gas accountancy and error calculation

As mentioned before, the time evolution of the amount of D_2 gas inside the chamber is calculated using the ideal gas law:

$$n = \frac{pV}{RT} \quad (4)$$

with n being the amount of D_2 (in mol), p, its pressure (in Pa), V, its volume (in m^3), $R = 8.314$ J K^{-1} mol^{-1}, the ideal gas constant, and T, the temperature of the gas (in K). Assuming only radiation from the top and bottom ("infinite") surfaces, T is determined with [27]:

$$T = \sqrt[4]{\frac{T_\alpha^4 + T_\beta^4}{2}} \quad (5)$$

where T_α and T_β, are the temperatures measured by RT-01 and RT-03, respectively (both in K).

The uncertainty assessment has been carefully tackled, attending to the systematic and random errors of each pressure and temperature sensor and following the general equation for error propagation [28]:

$$\delta f(x_i)^2 = \sum_{i=1}^{N} \left(\frac{\partial f}{\partial x_i}\right)^2 \delta x_i^2 \quad (6)$$

4. Results

4.1. Dissolution experiments: quantification of gas decrease (dissolved into Pb-Li and walls)

After the chamber containing the Pb-Li has been evacuated and thermalised, D_2 is injected for about one minute, until the required initial pressure is achieved. Once the valve is closed, the evolution of D_2 pressure (p) and temperature (T) during the dissolution run#01 is shown in Fig. 4. The gas pressure decreases as the deuterium diffuses into the Pb-Li and the stainless-steel walls. The gas temperature (T) is calculated with equation (5) and its thermalization takes around 4 h, as seen in Fig. 4. However, note that the variation in temperature is less than 2 K (in all runs), in comparison with the uncertainty (about ± 8 K), thus, the temperature can be considered constant during the whole dissolution experiment. The gas volume, $V_{gas} = (3.65 \pm 0.04) \times 10^{-3}$ m^3, is calculated by subtracting the chamber volume, $(4.88 \pm 0.02) \times 10^{-3}$ m^3, and the Pb-Li volume ($V_{PbLi} = 1.23 \times 10^{-3}$ m^3, in run#01). V_{PbLi} in the dissolution chamber slightly changes (< 5%) for each experiment due to the re-circulation of Pb-Li through the entire experimental setup between runs (as mentioned in Section 3.1). With the sensors RT-02 and RT-03 (see Fig. 1), the Pb-Li level would only be known for $h_{PbLi} = 20$ and 30 mm. Thus, a Matlab routine has been used to improve the accuracy (from ± 22% to ± 3%) of the Pb-Li height and volume. This routine is based on [29] and takes into account the full geometry of the setup, Pb-Li levels in the different parts and its flow, when transferring the Pb-Li between chambers. The volume of Pb-Li for each run in given in Table 3.

With p, T and V, the amount of gas, n, is calculated with equation (4). Over time, n decreases, and its slope also declines as the deuterium concentration increases in both the Pb-Li and the walls. However, even after the metals reach full saturation, the amount of gas continues to decrease due to permeation. A linear fit (solid black) performed to the last 24 h of the experiment shows that the amount of gas tends to a constant decrease, corresponding to the steady-state of the system.

The graphically-determined dissolution time, ultimately used for the calculations of $n_{D2[PbLi]}$, can be compared with estimations from theory, using the characteristic time scale of a diffusion process [30], $\tau_{diss} = h_{PbLi}^2 / (2D)$ (where h_{PbLi} is the height of Pb-Li in the chamber, and D, the diffusivity constant). For this assessment, it has been assumed that the atoms of deuterium only diffuse in the vertical direction, since the Pb-Li height is over an order of magnitude smaller than the internal diameter of the chamber ($h_{PbLi} \approx 22$ mm, $\varphi_{in} = 250$ mm). Considering a diffusivity $D = 3.14 \times 10^{-9}$ m^2 s^{-1}, which is the average between the values reported for deuterium by Edao et al. [16] and Reiter [12] at 673 K, a value $\tau_{diss} = 1392$ min (plotted in Fig. 4) is obtained, which is in agreement with the graphical interpretation.

This has been performed for all runs. Note that τ_{diss} delimits the start of a dynamic equilibrium in the Pb-Li, since p still decreases after τ_{diss}, the amount of dissolved D decreases according to Sieverts' law. This effect is taken into account later in Section 4.3.

In run#01, the initial pressure is $p_0 = 1023.4 \pm 1.1$ hPa and it decreases by $-\Delta p = 52.3 \pm 1.5$ hPa until τ_{diss}. The initial and final experimental values of p are determined with an average over 10 data points. The amount of gas lost until τ_{diss}, $-\Delta n = (3.51 \pm 0.12) \times 10^{-3}$ mol$_{D2}$, is determined as follows:

$$-\Delta n = (n_0 - n_f) = \frac{(p_0 - p_f)V}{RT} = \frac{-\Delta pV}{RT} \quad (7)$$

The calculated uncertainties of $-\Delta n$ are in the range of 3.2 – 5.4%, resulting from sensor precision and error propagation as described in 3.2.

4.2. Evaluation of D_2 lost through the walls

4.2.1. Permeation experiments (without Pb-Li)

Prior to the dissolution experiments, three permeation experiments were conducted before inserting the Pb-Li in the chamber, with the following two main objectives: (i) to determine experimentally how much deuterium is lost through the walls of the chamber, and (ii) to verify that the bake-out time between runs (as defined in 3.3) is enough to unload the walls of deuterium before the next experiment, ensuring the repeatability of the method.

Deuterium gas is injected in the previously evacuated and thermalised chamber for about one minute. After closing the valve, the evolution of the D_2 pressure and temperature during the first permeation experiment, perm#01, is shown in Fig. 5. The amount of gas loss through all the walls is evaluated at $t = 1392$ min (τ_{diss} of run#01) to be $(4.28 \pm 0.16) \times 10^{-3}$ mol$_{D2}$, which is $n_{D2[ss^*]}$ in Fig. 3 a). The resulting $n_{D2[ss^*]}$ values from all three permeation experiments have an uncertainty ranging from 3.7 to 5.6%, assessed as described in 3.2.

Fig. 6 shows the evolution of the amount of D_2 in the chamber during the permeation experiment perm#01 and its repetition, perm#02. The consistency between the results shows that the deuterium remaining in the walls from the previous experiment, after the bake-out process, is negligible in comparison with the experimental uncertainty.

4.2.2. Determination of gas lost through the non-wetted walls

This step involves a theoretical calculation of deuterium permeation through the chamber surfaces, in order to determine the theoretical fraction of D_2 lost through the non-wetted surfaces (identified as 1 and 2 in Fig. 3 b)). As shown in Fig. 3 b), the total permeation area is divided into four parts corresponding to different temperatures and thicknesses. The vertical wall is separated into two sections defined by the height of Pb-Li in the dissolution runs.

The amount of D_2 permeated though each surface is calculated with:

$$J = P(\sqrt{p_b} - \sqrt{p_a})A/\varepsilon \quad (8)$$

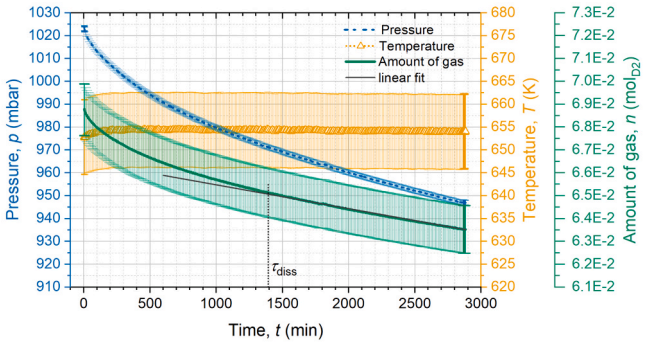

Fig. 4. Time evolution of D_2 pressure (p), temperature (T), and the calculated amount of gas (n) during the dissolution experiment run#01.

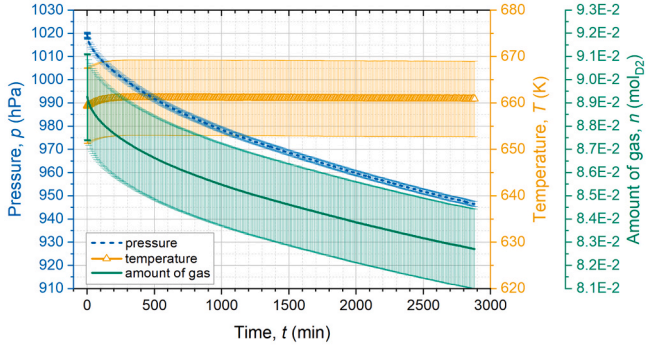

Fig. 5. Time evolution of D_2 pressure (p), temperature (T), and the calculated amount of gas (n) during the permeation experiment perm#01.

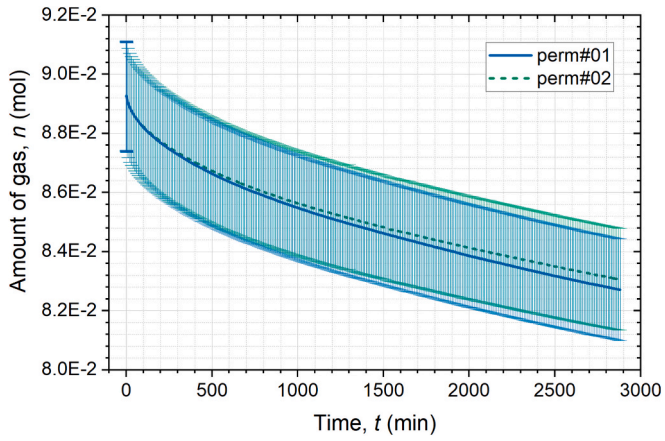

Fig. 6. Evolution of the amount of gas (n) during the permeation experiments perm#01 and perm#02.

where J is the flux of D atoms ($mol_D\ s^{-1}$), P is the permeability ($mol_D\ m^{-1}\ s^{-1}\ Pa^{-1/2}$), p_a and p_b are the partial pressures of D_2 at both sides of the wall (Pa), A is the permeation area (m^2), and ε is the wall thickness (m).

The left part of Table 2 (I) shows a summary of the values used in the calculations related to run#01 (area, thickness and temperature). The amount of permeated D_2 through the four surfaces is calculated with the two values of permeability reported in literature for deuterium (Shiraishi *et al.* [31] and Lee *et al.* [32]), and with the experimental temperatures and pressure of perm#01 during the τ_{diss} of run#01 (1392 min). These results are shown in the right part of Table 2 (II). The total theoretical permeation through all four surfaces, $(1.91 \pm 0.07) \times 10^{-3}$ mol_{D2} and $(1.21 \pm 0.04) \times 10^{-3}$ mol_{D2}, with permeabilities from [31] and [32] respectively, are smaller than the experimental value obtained in perm#01, $n_{D2[ss^*]} = (4.28 \pm 0.16) \times 10^{-3}$ mol_{D2}. The difference stems from the fact that theoretical calculations based on permeability assume steady-state conditions, whereas the experimental results also include the initial non-steady-state phase of D_2 permeation. This confirms the relevance to determine the amount of deuterium lost through the walls based on experimental values rather than (steady-state) theoretical permeation rates.

The fraction of permeation through the non-wetted area is determined to be (61 ± 3)% – (60 ± 4)% with the two P values (as shown in Table 2). The average, χ_{top}=(60 ± 2)%, is used to determine the amount of D_2 lost through the walls with equation (3). Therefore, in the dissolution run#01, the total amount of deuterium lost through the non-wetted walls is $n_{D2[ss]} = (60 \pm 2)\%\ (4.3 \pm 0.2) \times 10^{-3} = (2.6 \pm 0.1) \times 10^{-3}$ mol_{D2}.

It should be noted that the calculation of $n_{D2[ss]}$ relies on the following assumptions. First, the fraction of deuterium migrating through the different surfaces is constant in both the non-steady-state and the steady-state. Second, the permeation flux through the walls calculated with equation (8) has been treated using a 1D approximation, justified by the fact that the mass-transport perpendicular to the surface dominates. In this approach, a linear temperature gradient is assumed in the stainless-steel walls and simplified to an average value, as shown in Fig. 3 b).

4.3. Evaluation of deuterium dissolved in Pb-Li

The amount of deuterium dissolved in the Pb-Li, $n_{D2[PbLi]}$, is determined with the mass balance presented in equation (2) using the values of $-\Delta n_{D2}$ and $n_{D2[ss]}$, obtained in Sections 4.1 and 4.2, respectively. For run#01, the deuterium dissolved at τ_{diss} is $(9.3 \pm 1.5) \times 10^{-4}$ mol_{D2}. Since the dissolving pressure slightly decreases from 971.1 to 946.9 hPa between τ_{diss} = 1392 min and the end of the experiment (t_{end} = 2880 min), the amount of deuterium dissolved is corrected following the relation:

$$\frac{n_{D2[PbLi]}(t_{end})}{n_{D2[PbLi]}(\tau_{diss})} = \frac{C_D(t_{end})}{C_D(\tau_{diss})} = \frac{\sqrt{p_{D2}(t_{end})}}{\sqrt{p_{D2}(\tau_{diss})}} \quad (9)$$

resulting in $n_{D2[PbLi]}$ $(t_{end}) = (9.2 \pm 1.5) \times 10^{-4}$ mol_{D2}, at the end of run#01 (≈98.7% of the amount evaluated at τ_{diss}). The resulting values of $n_{D2[PbLi]}$ for all runs are given in Table 3.

It is important at this stage to compare the fraction of gas actually dissolved in the Pb-Li with the amount lost via permeation. From the total gas decrease during each dissolution experiment at τ_{diss} ($-\Delta n_{D2}$), only 21 – 31% is dissolved into the Pb-Li ($n_{D2[PbLi]}$), whereas the remaining 69 – 79% has permeated through the stainless-steel walls ($n_{D2[ss]}$). This underscores the importance of accurately quantifying permeation losses when assessing deuterium solubility in Pb-Li. More generally, it implies that if permeation is not prevented or accounted for while using stainless steel facilities, experimental values of hydrogen solubility in Pb-Li may be significantly overestimated.

Complementary to this experimental work, an estimation of the deuterium lost from the Pb-Li to the wetted surfaces has been assessed in a previous work [26] to be a 16% of the total deuterium that entered the Pb-Li during the dissolution experiments. This estimation lies within the

Table 3
Dissolution values evaluated at tend for each experiment. Final pressure of D_2 at the gas phase (p_{D2}), volume of Pb-Li in the dissolution chamber (V_{PbLi}), total amount of D_2 dissolved in the Pb-Li ($n_{D2[PbLi]}$), atomic concentration of deuterium in the liquid metal (C_D) and the Sievertsconstant (K_s) at 673 K.

Run	p_{D2} (hPa)	V_{PbLi} ($\times 10^{-3}$ m^3)	$n_{D2[PbLi]}$ ($\times 10^{-4}$ mol_{D2})	C_D (mol_D m^{-3})	K_s ($\times 10^{-3}$ mol m^{-3} $Pa^{-1/2}$)
#01	946.9 ± 1.1	1.23 ± 0.03	9.2 ± 1.5	1.5 ± 0.3	4.8 ± 0.8
#02	952.8 ± 1.1	1.18 ± 0.03	6.7 ± 1.5	1.1 ± 0.3	3.7 ± 0.8
#03	945.5 ± 1.1	1.20 ± 0.04	8.1 ± 1.6	1.4 ± 0.3	4.4 ± 0.9
#04	471.1 ± 1.1	1.19 ± 0.03	4.4 ± 1.3	0.7 ± 0.2	6.0 ± 0.8
#05	472.8 ± 1.1	1.24 ± 0.03	4.4 ± 1.4	0.7 ± 0.2	3.4 ± 1.0
#06	941.4 ± 1.1	1.25 ± 0.03	12 ± 2	1.9 ± 0.3	3.3 ± 1.0

Table 2
Theoretical D_2 permeation through the four chamber surfaces depicted in Fig. 3b), using the Pb-Li height in run#01. (I) Permeation parameters: area (A), thickness (ε) and temperature (T) during perm#01. (II) Theoretical calculations of D_2 permeated in perm#01 during 1392 min, with permeabilities (P) from [31,32]. Obtained percentage of D_2 permeated through the "non-wetted" and "wetted" surfaces in run#01 (in bold).

Permeation surface as in Fig. 3 b):	(I) Permeation parameters:				(II) Theoretical D_2 permeated (mol_{D2}):			
		A (m^2)	ε (mm)	T (K)	with P from [31]		with P from [32]	
non-wetted:	(1) upper flange	0.049	25	640 ± 10	$(6.0 \pm 1.2) \times 10^{-5}$	**(61 ± 3)%**	$(3.7 \pm 0.8) \times 10^{-5}$	**(60 ± 4)%**
	(2) non-wetted wall	0.057	2	653 ± 2	$(1.1 \pm 0.05) \times 10^{-3}$		$(6.9 \pm 0.3) \times 10^{-4}$	
wetted:	(3) wetted wall	0.018	2	677 ± 3	$(5.7 \pm 0.3) \times 10^{-4}$	**(39 ± 2)%**	$(3.7 \pm 0.2) \times 10^{-4}$	**(40 ± 2)%**
	(4) lower flange	0.049	20	689 ± 5	$(1.8 \pm 0.2) \times 10^{-4}$		$(1.2 \pm 0.1) \times 10^{-4}$	

experimental uncertainty of the presented results and therefore not included in the determination of K_s. It should nevertheless be kept in mind that not explicitly accounting for the D_2 lost from the Pb-Li to the wetted surfaces leads to a slight overestimation of the deuterium dissolved and the Sieverts' constant hereby determined.

4.4. Sieverts' constant

The average concentration of atomic deuterium in the Pb-Li, C_D, is calculated with the following equation and presented in Table 3:

$$C_D = 2\frac{n_{D2[PbLi]}}{V_{PbLi}} \quad (10)$$

As expected, the runs with similar dissolving pressure have similar $n_{D2[PbLi]}$ (t_{end}) and C_D (t_{end}). The solubility coefficient or Sieverts' constant (K_s) is evaluated from the experimental results, with Sieverts' law (equation (1)), using the dissolving pressure and concentration C_D both at t_{end}. The resulting values of K_s are given in Table 3 and are depicted in Fig. 7 for comparison with the literature values [6–20]. The six solubility values presented in this work exhibit a relative standard deviation of 25%, with individual relative uncertainties ranging from ± 13% to ± 30%. The average Sieverts' constant is $K_s = (4.3 \pm 1.1) \times 10^{-3}$ mol m^{-3} Pa$^{-1/2}$. The evaluated uncertainty, often overlooked in previous works, is relatively low compared to the several orders of magnitude dispersion of the Sieverts' constant reported values.

From previous studies [21,22], the wide dispersion in reported values of the Sieverts' constant (shown in Fig. 7) may be attributed to several factors: (i) the use of different experimental methods (typically absorption, desorption and permeation), (ii) the Li content of the Pb-Li alloy used, and/or (iii) the presence of impurities within the alloy. In particular, the influence of (ii) and (iii) are difficult to assess, since the composition of the Pb-Li used in the experiments (Li fraction and impurities) is often not verified. Instead, only the eutectic mixture provided by the manufacturer is reported.

The solubility determined in this study falls within the lower range of previously reported values obtained using absorption methods (depicted in blue in Fig. 7). This is attributed to the rigorous quantification of deuterium permeation through the chamber walls conducted in the present work.

The amount of deuterium lost through the 316 L stainless-steel walls during the dissolution experiments represents ≈ 69 − 79% of the total gas decrease. This underscores that permeation of hydrogen isotopes through stainless-steel containers or pipes is, not only non-negligible, but larger than the permeability of hydrogen isotopes in Pb-Li. Thus, hydrogen isotopes permeation is not only a safety issue (particularly in systems involving tritium), but also presents a challenge for any experiment, in which permeation can compete with the process that is studied.

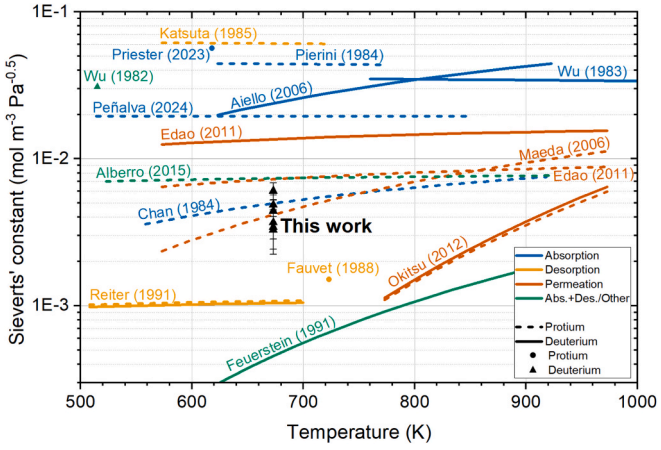

Fig. 7. Sieverts' constant values determined within the present work for deuterium dissolution in Pb-Li (15.2 at.% Li) at 673 K, in comparison with other reported values for hydrogen isotopes [6–20] The value plotted for Priester et al. represents the lower boundary reported in [19].

Furthermore, the Li content in the Pb-Li used in this work (15.2 ± 0.2 at.%) is slightly lower than that reported in other studies employing an absorption method, which typically range from 15.7 to 17 at.%, which may also explain a lower solubility [8,21].

The obtained results are close to the values reported by Chan *et al.* [8], Maeda *et al.* [15], Edao *et al.* [16] and Alberro *et al.* [18]. The latter, and most recent of the four, performed both absorption and desorption campaigns, and also did blank experiments to subtract the contribution of the experimental chamber walls and crucible.

The values reported by Priester *et al.* [19], which lie at the upper limit of those obtained by an absorption method, were measured using a different experimental setup and equilibrium pressures on the order of 0.1 mbar (four orders of magnitude lower than in the present work), due to tritium inventory constrains. The discrepancies between their results and the present work are therefore attributed to the possibility of working at another regime (with more effects of surface dynamics at lower pressures), as well as potential deviations in the lithium fraction, since the Pb-Li composition following the experiments was not reported.

The most recent experimental study by Peñalva *et al.* [20] also employed an absorption method, along with blank experiments to account for the contribution of hydrogen absorption by the experimental rig. Similar to the present work, their Pb-Li allow contained a lower Li fraction than the eutectic composition. Although they reported a higher solubility constant, the values obtained in this study fall within the standard deviation of their reported results.

5. Conclusions

In this work, the solubility of deuterium in Pb-Li was determined by a carefully designed experimental strategy using a mass balance, with a methodical evaluation of deuterium permeation into the structural materials and a rigorous uncertainty analysis, both rarely reported in the literature. Six experiments were conducted at different deuterium dissolution pressures, yielding consistent solubility values that follow Sieverts' law.

The experimental results include the quantification of dissolved deuterium and the corresponding Sieverts' constant, together with a composition analysis of the Pb-Li alloy (15.2 ± 0.2 at.% Li). The obtained amount of deuterium dissolved in Pb-Li, at 673 K, was (8.9 ± 1.5) × 10^{-4} and (4.4 ± 1.4) × 10^{-4} mol_{D2}, corresponding to dissolving pressures of 947 ± 5 and 472 ± 2 hPa, respectively. The average deuterium concentrations in Pb-Li at these pressures were 1.5 ± 0.3 and 0.7 ± 0.2 mol_D m^{-3}. The obtained Sieverts' constant, (4.3 ± 1.1) × 10^{-3} mol m^{-3} Pa$^{-1/2}$ at 673 K, is consistent with literature values and falls within the range reported by Chan *et al.* [8], Maeda *et al.* [15], Edao *et al.* [16], Alberro *et al.* [18], Peñalva *et al.* [20]. The given solubility assumes that no deuterium leaves the Pb-Li during the dissolution time, which is nevertheless justified since its impact on the here reported K_s values are estimated to remain within the experimental uncertainty.

This work provides an experimental solubility value together with a detailed description of the conditions under which it was obtained. It highlights the need to properly account for permeation effects (or to suppress them through coatings or alternative structural materials), which are often overlooked and may contribute to the discrepancies in reported K_s values. Other potential sources of discrepancies, such as the Pb-Li composition (Li fraction and impurities), also require investigation. In addition, possible isotope-dependent differences may need to be evaluated. These experimental efforts would benefit from complementary simulation support, for example through 2D or 3D modelling or multi-physics approaches.

CRediT authorship contribution statement

Ester Diaz-Alvarez: Writing – review & editing, Writing – original draft, Visualization, Validation, Software, Methodology, Investigation, Formal analysis, Conceptualization. **Rodrigo Antunes:** Writing – review & editing, Investigation, Conceptualization. **Stefan Welte:** Writing – review & editing, Resources, Conceptualization. **Laëtitia Frances:** Writing – review & editing, Supervision, Methodology, Investigation, Conceptualization.

Declaration of competing interest

The authors declare that they have no known competing financial interests or personal relationships that could have appeared to influence the work reported in this paper.

Acknowledgements

The authors would like to express their sincere gratitude to Prof. Robert Stieglitz, whose guidance and support were instrumental throughout the development of this work.

The Pb-Li chemical analyses were performed by T. Kaiser, P. Khelashvili and Dr. T. Bergfeldt, Chemical Analysis group, Institute for Applied Materials, KIT.

This work has been carried out within the framework of the EUROfusion Consortium and has received funding from the Euratom research and training programme 2014-2018 under grant agreement No 633053. The views and opinions expressed herein do not necessarily reflect those of the European Commission.

Data availability

Data will be made available on request.

References

[1] P. Arena, A. Del Nevo, J. Aktaa, G. Bongiovì, L. Bühler, I. Catanzaro, S. Cesaroni, G. Caruso, B. Chelihi, C. Ciurluini, A. Collaku, F. Colliva, C. Garnier, F. Giannetti, P. Haghdoust, V. Imbriani, F. Lucca, P. Maccari, L. Maqueda, L. Melchiorri, C. Mistrangelo, G. Mongiardini, F. Moro, T. Moulignier, R. Mozzillo, S. Noce, I. Pagani, J.B. Pontier, T. Pomella Lobo, M. Principato, P. Ruiz, L. Savoldi, S. Siriano, A. Tassone, F.R. Urgorri, F. Viganò, Á. Yañez, Design of the WCLL BB in view of the conceptual design phase, Fusion Eng. Des. 218 (2025) 115205, https://doi.org/10.1016/j.fusengdes.2025.115205.

[2] D. Rapisarda, I. Fernández-Berceruelo, A. García, J.M. García, B. Garcinuño, M. González, C. Moreno, I. Palermo, F.R. Urgorri, A. Ibarra, The European Dual Coolant Lithium Lead breeding blanket for DEMO: status and perspectives, Nucl. Fusion 61 (2021) 115001, https://doi.org/10.1088/1741-4326/ac26a1.

[3] F.A. Hernández, P. Arena, L.V. Boccaccini, I. Cristescu, A. Del Nevo, P. Sardain, G. A. Spagnuolo, M. Utili, A. Venturini, G. Zhou, Advancements in designing the DEMO driver blanket system at the EU DEMO pre-conceptual design phase: overview, challenges and opportunities, J. Nucl. Eng. 4 (2023) 565–601, https://doi.org/10.3390/jne4030037.

[4] D. Martelli, A. Venturini, M. Utili, Literature review of lead-lithium thermophysical properties, Fusion Eng. Des. 138 (2019) 183–195, https://doi.org/10.1016/j.fusengdes.2018.11.028.

[5] P. Hubberstey, T. Sample, M.G. Barker, Is Pb-17Li really the eutectic alloy? a redetermination of the lead-rich section of the Pb-Li phase diagram (0.0 < xLi(at%) < 22.1), Fusion React. Mater. Part A 191–194 (1992) 283–287, https://doi.org/10.1016/S0022-3115(09)80051-2.

[6] C.H. Wu, The solubility of deuterium in lithium-lead alloys, J. Nucl. Mater. 114 (1983) 30–33, https://doi.org/10.1016/0022-3115(83)90069-7.

[7] G. Pierini, A.M. Polcaro, P.F. Ricci, A. Viola, Solubility of hydrogen in the molten lithium-lead (Li17Pb83) alloy, J. Chem. Eng. Data 29 (1984) 250–253, https://doi.org/10.1021/je00037a007.

[8] Y.C. Chan, E. Veleckis, A thermodynamic investigation of dilute solutions of hydrogen in liquid Li-Pb alloys, J. Nucl. Mater. 123 (1984) 935–940, https://doi.org/10.1016/0022-3115(84)90198-3.

[9] H. Katsuta, H. Iwamoto, H. Ohno, Hydrogen solubility in liquid Li17Pb83, J. Nucl. Mater. 133–134 (1985) 167–170, https://doi.org/10.1016/0022-3115(85)90127-8.

[10] P. Fauvet, J. Sannier, Hydrogen behaviour in liquid 17Li83Pb alloy, J. Nucl. Mater. 155–157 (1988) 516–519, https://doi.org/10.1016/0022-3115(88)90301-7.

[11] R. Schumacher, A. Weiss, Hydrogen solubility in the liquid alloys lithium-indium, lithium-lead, and lithium-tin, Berichte Bunsenges. Für Phys. Chem. 94 (1990) 684–691, https://doi.org/10.1002/bbpc.19900940612.

[12] F. Reiter, Solubility and diffusivity of hydrogen isotopes in liquid Pb-17Li, Fusion Eng. Des. 14 (1991) 207–211, https://doi.org/10.1016/0920-3796(91)90003-9.

[13] H. Feuerstein, H. Gräbner, S. Horn, J. Oschinski, Transport of deuterium and rare gases by flowing molten Pb-17Li, J. Nucl. Mater. 179–181 (1991) 882–885, https://doi.org/10.1016/0022-3115(91)90230-5.

[14] A. Aiello, A. Ciampichetti, G. Benamati, Determination of hydrogen solubility in lead lithium using sole device, Fusion Eng. Des. 81 (2006) 639–644, https://doi.org/10.1016/j.fusengdes.2005.06.364.

[15] Y. Maeda, Y. Edao, S. Yamaguchi, S. Fukada, Solubility, diffusivity, and isotopic exchange rate of hydrogen isotopes in Li-Pb, Fusion Sci. Technol. 54 (2008) 131–134. https://doi.org/10.13182/FST54-131.

[16] Y. Edao, H. Noguchi, S. Fukada, Experiments of hydrogen isotope permeation, diffusion and dissolution in Li–Pb, J. Nucl. Mater. 417 (2011) 723–726, https://doi.org/10.1016/j.jnucmat.2010.12.126.

[17] H. Okitsu, Y. Edao, M. Okada, S. Fukada, Analysis of diffusion and dissolution of two-component hydrogen (H + D) in lead lithium, Fusion Eng. Des. 87 (2012) 1324–1328, https://doi.org/10.1016/j.fusengdes.2012.03.004.

[18] G. Alberro, I. Peñalva, A. Sarrionandia-Ibarra, F. Legarda, G.A. Esteban, Experimental determination of solubility values for hydrogen isotopes in eutectic Pb–Li, Fusion Eng. Des. 98–99 (2015) 1919–1923, https://doi.org/10.1016/j.fusengdes.2015.05.060.

[19] F. Priester, R. Größle, N. Bekris, I. Cristescu, A new facility for the measurement of the Sieverts'-constant for PbLi with tritium, Fusion Eng. Des. 191 (2023) 113568, https://doi.org/10.1016/j.fusengdes.2023.113568.

[20] I. Peñalva, M. Malo, M. Urrestizala, J. Azkurreta, N. Alegría, C. Moreno, D. Rapisarda, Experimental determination of the surface rate constants of protium and deuterium in Eurofer97, Nucl. Mater. Energy 38 (2024) 101618, https://doi.org/10.1016/j.nme.2024.101618.

[21] B. Garcinuño, R. Fernández-Saavedra, T. Hernández, M.B. Gómez, A. Quejido, D. Rapisarda, Establishing technical specifications for PbLi eutectic alloy analysis and its relevance in fusion applications, Nucl. Mater. Energy 30 (2022) 101146, https://doi.org/10.1016/j.nme.2022.101146.

[22] A. Pozio, M. Carewska, A. Santucci, S. Tosti, Behaviour of hydrogenated lead–lithium alloy, Int. J. Hydrog. Energy 42 (2017) 1053–1062, https://doi.org/10.1016/j.ijhydene.2016.08.166.

[23] E. Mas de les Valls, L.A. Sedano, L. Batet, I. Ricapito, A. Aiello, O. Gastaldi, F. Gabriel, Lead–lithium eutectic material database for nuclear fusion technology, J. Nucl. Mater. 376 (2008) 353–357, https://doi.org/10.1016/j.jnucmat.2008.02.016.

[24] E. Diaz-Alvarez, L. Frances, Accuracy evaluation and experimental plan of the Multi-Nozzle Vacuum Sieve Tray facility at the Tritium Laboratory Karlsruhe, Fusion Eng. Des. (2019), https://doi.org/10.1016/j.fusengdes.2019.03.074.

[25] Z. Köllő, C.G. Alecu, H. Moosmann, A new method to measure small volumes in tritium handling facilities, using p-V measurements, Fusion Sci. Technol. 60 (2011) 972–975. https://doi.org/10.13182/FST11-A12578.

[26] T. Pomella Lobo, E. Diaz-Alvarez, L. Frances, A model to simulate gas dissolution into/through metals and its application to deuterium in a 316L steel chamber with Pb-Li in a quasi-2D geometry, Appl. Sci. 12 (2022) 2523, https://doi.org/10.3390/app12052523.

[27] R. Siegel, Thermal radiation heat transfer, Fourth Edition, CRC Press, 2001.

[28] JCGM, Evaluation of measurement data — Guide to the expression of uncertainty in measurement JCGM 100:2008 GUM 1995 with minor corrections (https://www.bipm.org/utils/common/documents/jcgm/JCGM_100_2008_E.pdf), 2008. https://www.bipm.org/utils/common/documents/jcgm/JCGM_100_2008_E.pdf.

[29] M.A.J. Mertens, D. Demange, L. Frances, Model and simulation of a vacuum sieve tray for T extraction from liquid PbLi breeding blankets, Fusion Eng. Des. 112 (2016) 541–547, https://doi.org/10.1016/j.fusengdes.2016.05.038.

[30] E.J. Carr, Characteristic time scales for diffusion processes through layers and across interfaces, Phys. Rev. E 97 (2018) 042115, https://doi.org/10.1103/PhysRevE.97.042115.

[31] T. Shiraishi, M. Nishikawa, T. Yamaguchi, K. Kenmotsu, Permeation of multi-component hydrogen isotopes through austenitic stainless steels, J. Nucl. Mater. 273 (1999) 60–65, https://doi.org/10.1016/S0022-3115(99)00018-5.

[32] S.K. Lee, S.-H. Yun, H.G. Joo, S.J. Noh, Deuterium transport and isotope effects in type 316L stainless steel at high temperatures for nuclear fusion and nuclear hydrogen technology applications, Curr. Appl Phys. 14 (2014) 1385–1388, https://doi.org/10.1016/j.cap.2014.08.006.